Pergamon

Carbon Vol. 35, No. 3, pp. 427–436, 1997

0008-6223/97 $17.00 + 0.00

Mesoporous activated carbon filaments

W. Lu and D.D.L. Chung
Composite Materials Research Laboratory
State University of New York at Buffalo
Buffalo, NY 14260-4400

(Received 3 May 1996; accepted in revised form 17 December 1996)

Key Words - A. Activated carbon, B. Carbon filaments, C. Carbon fibers, D. surface area, porosity

In recent years, research on porous carbon materials has been very active. The forms of porous materials include the conventional activated carbon bulk [1-3], activated carbon fibers [4,5], fine carbon particles [6] and carbon aerogels [7]. Other than being used as adsorbents for purification and chemical processing [1-3], porous carbon materials are used as catalytic materials, battery electrode materials, capacitor materials, gas storage materials and biomedical engineering materials. A problem concerning this class of carbon materials relates to the need for high-surface-area porous carbons with mesopores and/or macropores, because such pores are desirable for gas (e.g., hydrogen) storage and capacitors, and many macromolecules and ions encountered in catalysis and batteries cannot penetrate the surface of the carbon without such pores. This paper introduces a new material that alleviates this problem.

According to IPUAC, pores are classified into four types, macropores (diam. > 500Å), mesopores (20Å < diam. < 500Å), micropores (8Å < diam. < 20Å) and micro-micropores (diam. < 8Å). Most pores are micropores in conventional activated carbons. The pore volume in activated carbon fibers (including pitch-based, PAN-based and rayon-based carbon fibers) is occupied by micropores (mainly) and micro-micropores. The pore volume in carbon aerogels is occupied by mesopores (mainly) and micropores. On the other hand, the specific surface areas of carbon aerogels are low (e.g., 650 m^2/g) [7] compared to activated carbons (as high as 3000 m^2/g). Furthermore, since this mesoporous carbon is in the form of ~0.1 μm diameter filaments, the separation between adjacent filaments in a filament compact is of the order of 0.1 μm, thus providing macropores within the compact. These elongated macropores serve as channels that facilitate fluid flow. The combination of mesopores within each filament and macropores between the filaments is in contrast to carbon aerogels, which have micropores within each particle and between particles and mesopores between chains of interconnected particles.

Carbon filaments of diameter ~0.1 μm (in contrast to a typical diameter of 10 μm for conventional carbon fibers), as grown catalytically from carbonaceous gases, are a relatively new type of carbon fiber [8-19]. Their applications include vibration damping [20], electromagnetic interference (EMI) shielding [21] and battery electrodes [22-24]. The activation of carbon filaments had not been previously reported. By activating carbon filaments of diameter ~0.1 μm, this work provides a mesoporous carbon with a high specific surface area. The attraction of this carbon for electrochemical application and for eletromagnetic interference shielding is the subject of companion papers.

Carbon filaments of diameter ~0.1 μm and with low crystallinity (as indicated by an extremely weak 002 graphite x-ray diffraction peak) were provided by Applied Sciences, Inc. (Cedarville, Ohio). They were grown from methane using an iron catalyst. They were bent, resembling cotton wool, with lengths at least 100 μm. Activation of the filaments was achieved by (i) drying at 110°C in air for 1 h, (ii) surface oxidation by exposing to O_3 gas (0.3 vol. %, in air) for 3 min. (can be from 2 to 10 min.) at 150°C, (iii) heating in N_2 to 500°C at 2°C/min., (iv) heating in N_2 to either 970 or 1000°C at 3°C/min., and (v) activation (primarily involving the reaction $C + CO_2 \rightarrow 2CO$) by heating in $CO_2 + N_2$ in 1:1 volume ratio (can be pure CO_2) at either 970 or 1000°C (can be from 900 to 1100°C) for 20-100 min. Step (ii) raised the surface oxygen concentration from 1.0 to 2.2 at.% (as shown by O_{1s} and C_{1s} peaks in ESCA), thereby enhancing activation in step (v), which further raised the surface oxygen concentration to 4.0 at.%. Table 1 shows the fractions of surface carbon atoms bonded to hydrogen as C-H (e.g., $(CH_2)_n$), bonded to oxygen as C-O (e.g., C-OH, C-O-C) and bonded to oxygen as C=O (e.g., O=C-OH, O=C-O-R), as shown by binding energy analysis in ESCA. No catalyst was detected by ESCA, indicating that the residual catalyst was not exposed. Ozone exposure increased the C-O fraction, but did not affect the C=O fraction. Activation increased both C-O and C=O fractions. In spite of the presence of the residual iron catalyst at the tip of each filament, step (ii) was

Table 1. Fractions of surface carbon atoms bonded as C-H, C-O and C=O

	C-H	C-O	C=O
As-received	94.0%	6.0%	0
After O_3 exposure	89.0%	11.0%	0
After activation	82.1%	13.4%	4.5%

Table 2. Specific surface area, pore size and pore volume of carbon filaments before and after activation.

Activation condition	Specific surface area (BET, m^2/G)	Pore size (Å)	Pore volume (cm^3/g)			Yield (%)
			Total	Lower size range[a]	Upper size range[b]	
As-received	54.0 ± 0.3	81.7*	0.110	0.061	0.049	/
After O_3 exposure	40.7 ± 0.3	99.1+	0.095	0.041	0.055	100
970°C, 20 min.	218 ± 2	55.2+	0.257	0.091	0.166	76.4
1000°C, 20 min.	532.5 ± 8.5	52.6+	0.575	0.112	0.463	/
970°C, 40 min.	913 ± 16	55.0+	1.077	0.204	0.873	56.2
970°C, 60 min.	1121 ± 8	55.3+	1.323	0.249	1.074	48.2
970°C, 80 min.	1306 ± 16	55.3+	1.548	0.267	1.280	36.2
970°C, 100 min.	1214 ± 11	54.1+	1.493	0.257	1.236	30.1

* Mean pore size from 10 to 1000 Å.
\+ Main pore size above 20 Å.
[a] Size below ~ 30 Å. See Fig. 1.
[b] Size above ~ 30 Å. See Fig. 1.

needed in order to attain a high specific surface area. Moreover, step (ii) is a surface treatment which served to minimize the mechanical property degradation during subsequent activation.

Table 2 shows the specific surface area (BET), pore size and pore volume (BJH for pore size > 20 Å and t-plot for pore size ≤ 20 Å [25]) of the filaments before and after the steps of activation treatment, as determined by nitrogen adsorption and measurement of the pressure of the gas during adsorption using the Micromeritics ASAP 2000 instrument. Even in the as-received condition, the filaments had mesopores, though the specific surface area was low. The mesopore size was slightly increased and the specific surface area was slightly decreased by the O_3 exposure, probably because this caused the removal of some surface microcracks, as O_3 is known to react with graphite [26]. Activation subsequent to O_3 exposure greatly increased the specific surface area and decreased the mesopore size, such that the specific surface area increased sharply with increasing activation time up to 80 min. at a fixed activation temperature (970°C) and the pore size was quite independent of the activation time. The specific surface area decreased slightly upon increasing the activation time from 80 to 100 min., probably due to the partial destruction of the pore structure at the high degree of activation corresponding to the activation time of 100 min. Fig. 1 shows the pore size distribution of the activated carbon filaments with the highest specific surface areas in Table 2. The pore size distribution was bimodal, with mesopores of mean size 55 Å dominating micropores of mean size 16 Å. A bimodal pore size distribution was observed for all activated filaments of Table 2, but not for the as-received or ozone treated filaments. Fig. 2 shows the nitrogen (77 K) adsorption/-desorption isotherms for the sample of Fig. 1. These

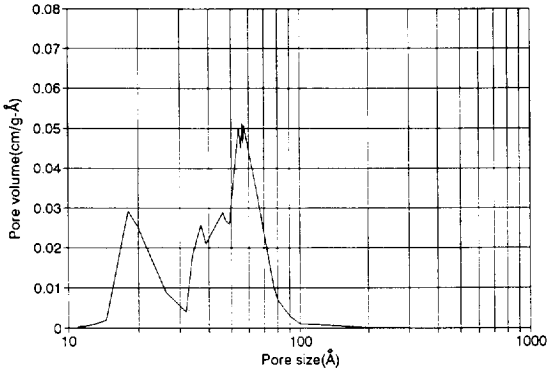

Fig. 1. Pore size distribution of activated carbon filaments with the largest specific surface area in Table 2.

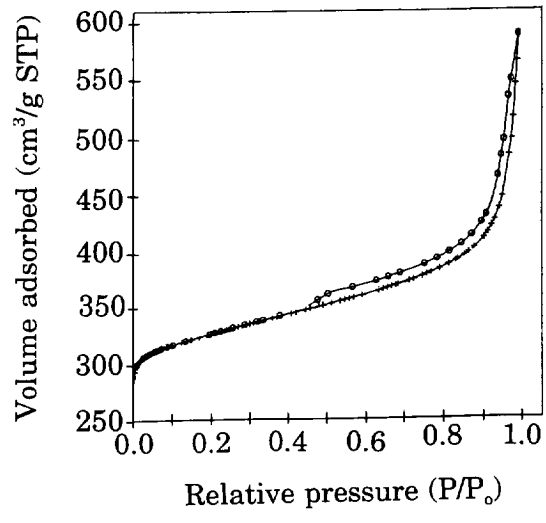

Fig. 2. Nitrogen adsorption (+) and desorption (o) isotherms for activated (970°C, 80 min.) carbon filaments.

isotherms are consistent with the bimodal pore size distribution in Fig. 1. The iodine adsorption of the sample of Fig. 1 was 1412.2 mg/g and the methylene blue decoloring was 256.4 ml/g, as measured with conventional techniques.

In order to measure the burn-off (fractional weight loss, or 1 - yield) due to activation, thermogravimetric analysis (TGA) using the Perkin-Elmer Co. (Norwalk, CT) TGA7 instrument was conducted after O_3 exposure under the same conditions as steps (iii), (iv) and (v) described above, such that the temperature was 970°C in steps (iv) and (v). The burn-off relative to the filament weight after step (ii) was 1.01%, 2.71%, 4.96% and 12.3% at 500, 600, 700 and 970°C, respectively, in steps (iii) and (iv), and 23.0%, 43.8%, 51.8%, 63.8% and 69.9% at 20, 40, 60, 80 and 100 min., respectively, in step (v). The sample with the largest specific surface area in Table 2 (970°C, 80 min.) corresponds to a burn-off of 63.8%, i.e., a yield of 36.2%. Fig. 3. shows the increase of the specific surface area and the decrease of the yield as the activation time was increased at a fixed activation temperature of 970°C.

The as-received carbon filaments had mesopores, though the specific surface area was not high. This is in contrast to conventional carbon fibers, which have essentially no pores. The porous nature of the filaments is attributed to the fact that the filaments are made from carbonaceous gases. Activation by CO_2 greatly increased the specific surface area.

X-ray diffraction using CuKα radiation showed that the d spacing for the graphite 002 plane was 3.367 Å and 3.476 Å for the as-received carbon filaments and the activated (970°C, 80 min.) carbon filaments respectively.

Thermogravimetric analysis (Perkin Elmer Co. TGA7) in air with a heating rate of 5°C/min (Fig. 4) showed that the activated (970°C, 80 min.) carbon filaments were thermally stable up to 451°C, at which point weight loss began due to oxidation of the carbon.

In summary, mesoporoous activated carbon filaments with a main pore size (BJH) 55 Å, specific surface area 1310 M^2/g, total pore volume 1.55 cm^3/g, and 83% of total pore vol. being pores of size > 30 Å, were obtained by activating catalytically grown carbon filaments of diameter ~0.1 μm in $CO_2 + N_2$ (1:1) at 970°C for 80 min. The yield was 36%. Prior to activation, the filaments were surface oxidized by exposure to ozone. The activated filaments exhibited a bimodal pore size distribution, with the upper size class

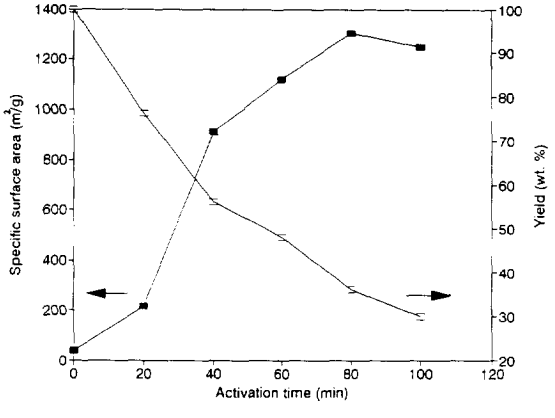

Fig. 3. Variation of specific surface area and yield with activation time for a fixed activation temp. of 970°C.

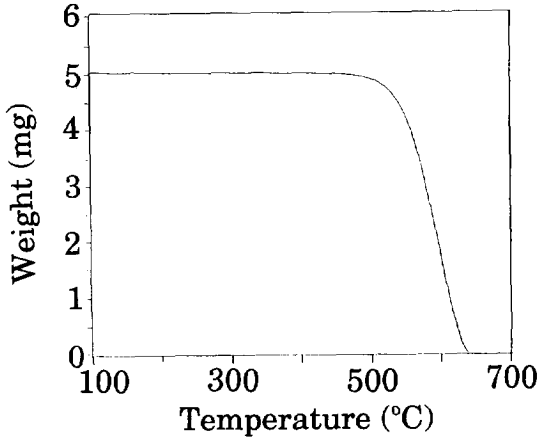

Fig. 4. Thermogravimetric analyses for activated (970°C, 80 min.) carbon filaments upon heating in air at 5°C/min.).

(> 30 Å) dominating. The as-received filaments had a mean (10-1000 Å range) pore size of 82Å, but the specific surface area was only 54 m^2/g. The specific surface area increased greatly with activation time (20-80 min.), but the main pore size essentially did not change with activation time. The activated filaments were thermally stable up to 451°C.

REFERENCES

1. Dubinin, M.M., Polyakov, N.S., and Petukhova, G.A., *Adsorption Science Tech.*, 1993, **10**(1-4), 17.
2. Chiang, H.-L., Chiang, P.C. and You, J.H., *Toxicological Environmental Chem.*, 1995, **47**(1-2), 97.
3. Takeuchi, Y. and Itoh, T., *Sep. Technol.*, 1993, **3**(3), 168.
4. Alcaniz-Monge, J., Cazorla-Amoris, D., Linares-Solano, A., Yoshida, S. and Oya, A., *Carbon*, 1994, **32**, 1277.
5. Oya, A., Yoshida, S., Alcaniz-Monge, J., Linares-Solano, A., *Carbon*, 1996, **34**, 53.
6. Chosal, R., Kaul, D.J., Boes, U., Sanders, D., Smith, D.M., and Maskara, A., *Advances in Porous Materials*, Materials Research Society Symp. Proc., 1995, Vol. 371, pp. 413-423.
7. Fung, A.W.P., Wang, Z.H., Lu, K., Dresselhaus, M.S. and Pekala, R.W., *J. Mater. Res.*, 1993, **8**, 1875.
8. Tennent, H.G., Barber, J.J. and Hoch, R., U.S. Patent 5,165,909. 1992.
9. Tibbets, G.G., *Carbon*, 1989, **27**, 745.
10. Ishioka, M., Okada, T., Matsubara, K. and Endo, M., *Carbon*, 1992, **30**, 865.
11. Smith, D.J., McCartney, M.R., Tracz, E. and Borowiecki, T., *Ultramicroscopy*, 1990, **34**(1-2), 54.
12. Kepinski, L., *React. Kinet. Catal. Lett.*, 1989, **38**, 363.
13. Kato, T., Haruta, K., Kusakabe, K., and Morooka, S., *Carbon*, 1992, **30**, 989.
14. Gadelle, P., in *Carbon Fibers, Filaments and Composites*, ed. J.L. Figueiredo, C.A. Bernardo, R.T.K.Baker and K.J. Hüttinger, Kluwer Academic, Dordrecht, 1990, pp. 95-117.
15. Ishioka, M., Okada, T., Matsubara, K. and Endo, M., *Carbon*, 1992, **30**, 859.
16. Baker, R.T.K. in *Carbon Fibers, Filaments and Composites*, ed. J.L. Figueiredo, C.A. Bernardo, R.T.K.Baker and K.J. Hüttinger, Kluwer Academic, Dordrecht, 1990, pp. 405-439.
17. Tibbetts, G.G., ibid. pp.525-540.
18. Sacco, A., Jr., ibid. pp. 459-505.
19. Motojima, S., Kawaguchi, M., Noxaki, K. and Iwanaga, H., *Carbon*, 1991, **29**, 379; *Appl. Phys. Lett.*, 1990, **56**, 321.

20. Hudnut, S.W. and Chung, D.D.L., *Carbon*, 1995, **33**, 1627.
21. Shui, X. and Chung, D.D.L., *J. Electron,. Mater.*, 1995, **24**, 107.
22. Shui, X. and Chung, D.D.L., *Carbon*, 1995, **33**, 1681.
23. Frysz, C.A., Shui, X. and Chung, D.D.L., *J. Power Sources*, 1996, **58**, 41.
24. Frysz, C.A., Shui, X. and Chung, D.D.L., *J. Power Sources*, 1996, **58**, 55.
25. Schneider, P., *Appl. Catalysis*A, 1995, **129**, 157.
26. Hennig, G.R., in *Chemistry and Physics of Carbon*, ed. P.L. Walker, Jr., Vol. 2, 1996. Dekker, New York, pp. 35-38.

Tribological properties of $FeCl_3$-graphite intercalation compound rubbed film on steel

T. JUN and X. QUNJI
Laboratory of Solid Lubrication, Lanzhou Institute of Chemical Physics
Chinese Academy of Sciences, Lanzhou 730000, P.R. China

(Received 5 May 1995; accepted in revised form 17 December 1996)

Key Words - A. Intercalation compounds, D. friction

It has been suggested that the low friction coefficient produced by graphite lubrication is due to the surface orientation of crystallites and the subsequent formation of lubricating rollers [1]. The surrounding environment influences the friction behavior [2-3]. It is known that atomic or molecular species can be inserted between the graphite layers, increasing the interplanar distance and thus weakening the bonds between these layers. The obvious application of this effect, which appears to have been overlooked, is to produce improved lubricating solids [4-5]. In this work, the tribological characteristics of a graphite intercalation compound (GIC) rubbed film on steel surfaces were evaluated with three machine tests. The structures of the rubbed films on the steels were then investigated in an attempt to explain the tribological behavior.

Natural graphite flake produced by Nanshu in China (purity: C content 97.46%) was used in this work. The average flake diameter is 4 μm and the crystallites are highly oriented (Fig. 1). In addition, the crystallite size (L_c), calculated from the (002) x-ray diffraction line width is about 150-160 Å.

A $FeCl_3$-GIC ($C/FeCl_3$=17/1) was prepared by adding the graphite flake to a solution of dehydrated $FeCl_3/CH_3NO_2$ at 50°C and refluxing for 5h. The product was washed with distilled water, filtered and kept in a desiccator at room temperature. The compounds were identified by x-ray diffraction. It therefore appears that they contain small amounts of free graphite and $FeCl_3$, and an enriched ferric chloride graphite intercalation compound phase (7.95 Å, 4.04 Å, 3.22Å). This product indicates the third stage (d=16.25Å) compound (Fig. 2a), with a crystallite size (L_c) of 627Å. The electron diffraction pattern seems to result from diffraction from a mixture of graphite and ferric chloride of (300) (d=179Å) and (110) (d=3.05Å) (Fig. 2b) TEM observation shows the basal plane as 100Å "islands" (Fig. 2c). All evidence supports the picture of a ferric chloride single layer intercalated between successive planes of carbon [6]. TG-DTA indicates that the compound deintercalates slowly at room temperature and decomposes rapidly at 420°C [7]. The metal surfaces were polished to a surface finish of 0.15 μm CLA (center line average) in random directions and then washed with acetone.

The graphite and GIC powders were reciprocatively rubbed onto the steel surfaces (AISI 1045 and AISI 305) at a rubbing velocity of 0.2 m/s and under a pressure of 2 x 10^4 Pa for various distances. The friction coefficient of the rubbed film in air was determined by a Kyowa drive friction precise measuring apparatus (DFPM), for which the block sample of the covered films moved against a stationary AISI-C-52100 steel ball (diameter 3 mm) at a velocity of 0.58 mm/s under a load of 0.49N. The endurance life of the rubbed film was evaluated with a HQ-1 friction and wear machine in air (such as the Timken machine), using an AISI-C-52100 ring of diameter 49.2 mm rotated against

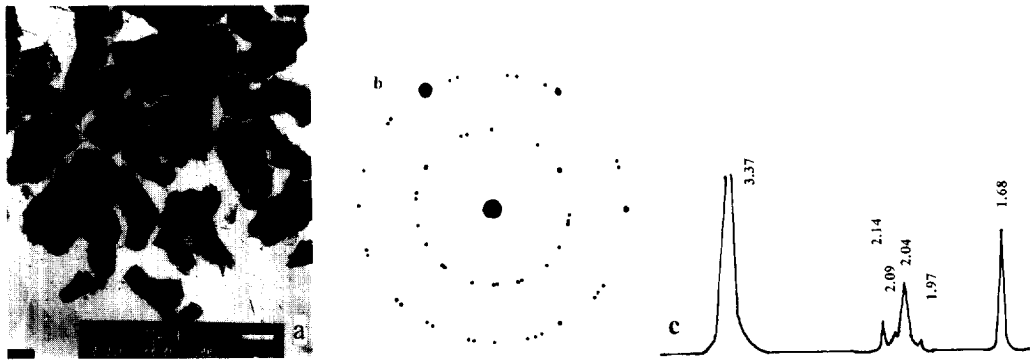

Fig. 1. (a) TEM (b) electron diffraction and (c) x-ray diffraction of Nanshu graphite flake.